

# A new resonant-based sensor for non-invasive measurement of blood glucose levels

Abolfazl Bijari, Faezeh Foolad, Mohammadreza Khorshidi

Department of Electronics, Faculty of Electrical and Computer Engineering, University of Birjand, Birjand, Iran

## Article Info

### Article history:

Received Apr 16, 2024

Revised May 18, 2025

Accepted May 26, 2025

### Keywords:

Blood glucose level

Dual-mode

Microwave sensor

Non-invasive

Resonator

Sensitivity

## ABSTRACT

This paper presents a rapidly developed non-invasive microstrip sensor for measuring blood glucose levels (BGLs). The sensor features a microstrip closed-loop square resonator integrated with an interdigital capacitor (IDC), creating a sensitive area for glucose detection when a patient's finger is placed on it. Using odd and even mode analytical methods and transmission line theory, we analyzed the sensor's performance. Results indicate that the second even mode demonstrates significant changes across a standard glucose concentration range. The sensor was designed and simulated in ANSYS high-frequency structure simulator (HFSS), showing a resonance frequency shift of up to 24.9 MHz at 1.94 GHz and a sensitivity of 110 kHz per mg/dL over a detection range of 0 to 216 mg/dL. Additionally, the frequency shift exhibits a high linear correlation (0.9485). In summary, the proposed sensor shows significant promise for achieving precise measurements of BGLs.

*This is an open access article under the [CC BY-SA](https://creativecommons.org/licenses/by-sa/4.0/) license.*



## Corresponding Author:

Abolfazl Bijari

Department of Electronics, Faculty of Electrical and Computer Engineering, University of Birjand

Birjand, Iran

Email: a.bijari@birjand.ac.ir

## 1. INTRODUCTION

Recently, there has been a growing demand for fast, inexpensive, sustainable, small, and highly sensitive sensing devices for various healthcare and biomedical applications. Precise and real-time monitoring of electrolytes and other physiological biomarkers in bodily fluids is crucial for effective evaluation of treatment advancements, rapid clinical diagnosis, and continuous observation [1]. This is especially critical for widespread conditions such as diabetes, whose prevalence is rising, particularly among populations with sedentary habits and high obesity rates. As reported by the International Diabetes Federation (IDF) [2], more than 400 million individuals globally are affected by diabetes, and its incidence continues to grow at differing rates annually. Many research studies show that patients with diabetes can easily avoid any series condition using continuous blood glucose monitoring. Precise monitoring of blood glucose levels (BGLs) is crucial for effective treatment, as maintaining these levels within the normal range of 50 to 200 mg/dL is vital [3]. Hönes *et al.* [4] proposed a highly accurate and reliable glucose-monitoring technique based on an electrochemical reaction. However, this method destroys the blood samples. Numerous studies have demonstrated that continuous blood glucose monitoring can help diabetic patients avoid serious complications. Presently, there is a rapidly growing interest in non-invasive and pain-free glucose monitoring methods that do not require long-term replacements [5]. Consequently, numerous topologies and methods have been developed, leveraging photoacoustic spectroscopy, optical spectroscopy, nanomaterial-based sensing, and electromagnetic sensing technologies [6]. The creation of a dependable non-invasive glucose monitoring system has the potential to significantly improve the quality of life for people with diabetes by eliminating the discomfort linked to conventional fingerstick

techniques. This advancement could encourage more frequent and less daunting monitoring, ultimately enhancing glycemic management and overall health outcomes.

Among the various non-invasive techniques studied, electromagnetic sensing methods have been found to be more advantageous than others. This is attributed to their straightforward fabrication, affordability, and the non-invasive characteristics of electromagnetic signals as they propagate through biological tissues. Unlike ionizing energy sources such as X-rays, which can pose potential health risks, electromagnetic signals are safer and do not cause harmful effects. Electromagnetic sensing techniques are based on detecting variations in the relative permittivity of blood as glucose levels fluctuate. These changes lead to slight shifts in the frequency response of the sensor, which can be measured and analyzed [7]–[10]. The relationship between the relative permittivity of blood and BGLs has been investigated, and it has been demonstrated that the relative permittivity of blood changes with variations in BGL [11], [12]. Yilmaz *et al.* [12] reported that the standard range for BGLs is 72 mg/dL to 216 mg/dL and showed that increasing BGLs decreases the relative permittivity of blood. Among the electromagnetic sensing methods, resonant-based techniques have gained popularity due to their high reliability and accuracy. They are also immune to noise and other measurement losses [13]. These sensors employ different types of resonators, such as transmission line (TL), closed-loop, and split or ring structures. Additionally, they are fabricated in various topologies of metal/dielectric cavities and metamaterial structures [9]. In these sensors, resonance properties such as resonance frequency, magnitude [14], phase [15], and quality factor [8] can be monitored when the resonator is unloaded. The resonator's frequency response shifts as a result of its field interactions with the material under test (MUT) at the resonance frequency. Consequently, the dielectric properties of the MUT can be determined by analyzing changes in the resonance response [16]. It is important to note that this method is particularly effective for characterizing low-loss materials within a narrow frequency range. For broader frequency analysis, harmonic resonance frequencies are utilized. Various reflection and/or transmission techniques have been applied to measure dielectric permittivity and blood glucose-related losses in superficial vessels, employing different types of resonators [17], antennas [18], or waveguides [19]. However, many of these microwave sensors tend to be costly, intricate, and large in size, rendering them impractical for direct, everyday use by diabetic patients in home settings.

A modified split ring resonator (SRR) is used to measure the glucose concentration at 2 GHz [20]. The sensor is investigated in different electrical and magnetic couplings and measures the glucose level changes by frequency and magnitude variation. The sensor exhibits a 0.8 kHz frequency shift per mg/dL of glucose level changes. Kim *et al.* [21] combined a spiral inductor and interdigital capacitor (IDC) to measure the glucose level in the blood plasma. The resonance frequency of the sensor is shifted up by increasing the glucose level in the blood plasma and exhibited a sensitivity of 1.99 MHz per mg/dL. Govind and Akhtar [22] improved the sensitivity of the SRR-based sensor by integrating it with the IDC and the microfluidic channel. A non-invasive and compact microwave blood glucose sensor is reported in [23]. The sensor used the fingertip for the measurements and exhibited a linear frequency shift of 14 MHz over the BGLs from 0 mg/dL to 1000 mg/dL. Kumar *et al.* [24] presented a highly sensitive complementary split-ring resonator (CSRR)-based microwave sensor. The sensor is comprised of a differential inductor and a centre-loaded circular IDC. The sensor is compact and fabricated on a GaAs substrate using a micromachining process and exhibits a high sensitivity of 1.175 MHz per mg/dL. A low-cost microwave sensor is demonstrated on an FR4 substrate based on the magnitude and resonance frequency of scattering parameters [25]. The sensor consists of an IDC embedded in a coplanar waveguide (CPW) line and shows a sensitivity of 2.353 kHz per mg/dL. However, most of the aforementioned studies on resonant-based glucose sensors are invasive and use an aqueous solution for measuring BGLs. Singh *et al.* [26] introduce an innovative design for a planar antenna-based sensor operating within the 5.8 GHz Industrial, Scientific, and Medical (ISM) band. This sensor utilizes RF wave technology, resulting in enhanced sensitivity and precision. Mohammadi *et al.* [27] utilize a branch line coupler directly linked to a split ring resonator (SRR) to create a sensor characterized by high sensitivity and a compact form factor. To prevent direct contact between the MUT and the sensor, a cover glass is placed over the sensing region. The reduction in size is accomplished through the inductive and capacitive properties of the SRRs. Variations in transmission zeros (TZs) were observed in response to different BGL.

This paper introduces a novel design for a non-invasive blood glucose sensor utilizing a dual-mode resonator, aimed at enabling feasible fabrication and enhancing sensitivity for human BGL detection. The paper is structured as follows: Section 2 provides a detailed explanation of the design process, electrical modeling, and analytical simulation of the proposed sensor. Section 3 presents and discusses the electromagnetic (EM) simulations conducted for blood glucose sensing. Finally, section 4 summarizes the findings and draws conclusions.

## 2. METHOD OF SENSOR DESIGN

The development of a microstrip resonant-based sensor for the non-invasive measurement of BGLs involves a series of systematic steps grounded in fundamental engineering principles. At the core of this design

is the resonant principle, which employs a microstrip resonator that modifies its resonant frequency in response to fluctuations in glucose concentrations, thereby capitalizing on the dielectric properties inherent to glucose solutions. The permittivity of the MUT can affect both the phase and amplitude of electromagnetic traveling waves passing through it. Therefore, microwave sensors measure the relative permittivity at a specific frequency. Table 1 presents the standard range of BGLs and the corresponding blood relative permittivity over the frequency range of 1 GHz to 10 GHz. Recent studies have shown that the relative permittivity of blood decreases as BGLs increase [12], [28].

Table 1. Dielectric properties of under-studying blood samples [12]

Tissue type	Blood glucose level (mg/dL)	Relative permittivity	Conductivity (S/m)
Blood 1 (0 g Dextrose)	0	59.5	2.5
Blood 2 (0.14 g Dextrose)	72	58.5	2.5
Blood 3 (0.24 g Dextrose)	126	57	2.5
Blood 4 (0.34 g Dextrose)	162	55.5	2.5
Blood 5 (0.44 g Dextrose)	216	54	2.5

Material selection is critical; appropriate substrates, such as FR-4, PTFE, or Rogers materials, are chosen for their advantageous dielectric characteristics and stability, while conductive materials like copper or gold are utilized for the microstrip traces due to their superior electrical conductivity. The design process typically encompasses the creation of either a microstrip patch antenna or a meander line resonator, with precise dimensions optimized to resonate at frequencies that are sensitive to variations in glucose levels, usually within the GHz range. To guarantee optimal performance, simulation software tool such as high-frequency structure simulator (HFSS) is employed to model the electromagnetic behavior of the resonator, facilitating a comprehensive analysis of how changes in glucose concentration affect the resonant frequency.

### 2.1. Proposed microstrip sensor

The design procedure is primarily inspired by the geometric design of a microstrip dual-mode resonator. Figure 1 shows the layout of the proposed resonator. As can be seen, the dual-mode resonator consists of a closed-loop square resonator loaded with an IDC, and the coupled lines are used as the input and output (I/O) feed lines. The resonator is designed on a Rogers\_RO6010 substrate with a relative dielectric constant  $\epsilon_r=10.2$ , loss tangent  $\delta=0.0023$ , and thickness of 0.254 mm.

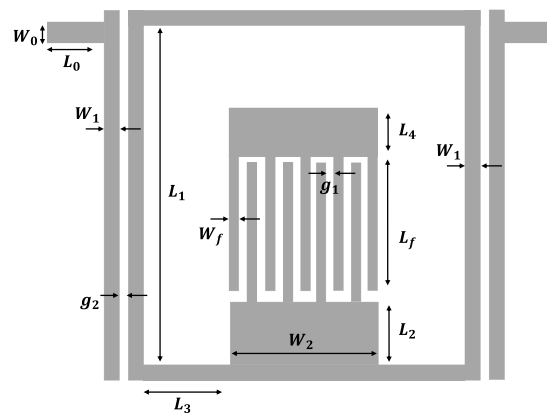


Figure 1. The layout of the proposed dual-mode resonator

### 2.2. Resonator characteristics

Since the proposed structure of the dual-mode resonator is symmetric, the even/odd mode excitation method can be used to characterize the resonance frequencies. Figures 2 and 3 (Figure 2(a) and Figure 3(a)) show the odd and even mode equivalent circuit models, respectively. Based on the odd-mode transmission line model illustrated in Figure 2(b), the input admittance for this mode ( $Y_{in,o}$ ) is derived as (1).

$$Y_{in,o} = -\frac{j(\tan\theta_{1d} + \tan\theta_{1u})}{Z_1(\tan\theta_{1d}\tan\theta_{1u})} \quad (1)$$

where  $Z_i$  and  $\theta_i$  are the characteristic impedance and effective electrical length, respectively.

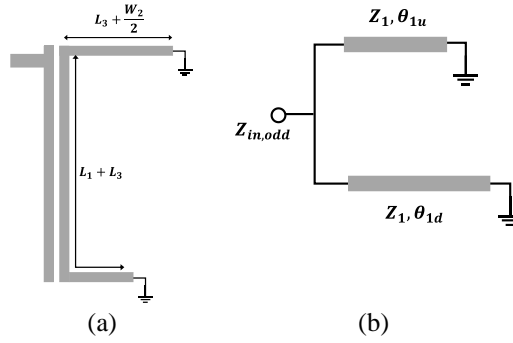


Figure 2. Equivalent circuit model of proposed resonator for odd mode: (a) electrical wall and (b) equivalent transmission line model

Assuming  $\theta_{1u} = \beta(L_3 + W_2/2)$  and  $\theta_{1d} = \beta(L_1 + L_3)$ , the resonance condition for the odd modes is derived by setting  $Y_{in,o} = 0$  as:

$$f_{r,o} = \frac{nc}{L_1 \sqrt{\epsilon_{eff}(4\alpha_1 + \alpha_2 + 2)}}; n = 1, 2, 3, \dots \quad (2)$$

where  $c$  represents the speed of light,  $\epsilon_{eff}$  is the effective dielectric constant of the microstrip substrate, and  $\alpha_1 = L_3/L_1$ , and  $\alpha_2 = W_2/L_1$ . By choosing  $L_1 = 20$  mm,  $\alpha_1 = 0.5$ , and  $\alpha_2 = 0.35$ , the fundamental odd resonance frequency of the proposed resonator lies at 1.25 GHz. Similarly, the input admittance for the even mode ( $Y_{in,e}$ ) can be derived from the transmission line model presented in Figure 3(b) as (3).

$$Y_{in,e} = \frac{1}{Z_{u,e}} + \frac{1}{Z_{d,e}} \quad (3)$$

where  $Z_{u,e}$  and  $Z_{d,e}$  denote the input impedances seen at the upper path and lower path, respectively, given by (4) and (5).

$$Z_{u,e} = -\frac{jZ_1}{\tan\theta_{1u}} \quad (4)$$

$$Z_{d,e} = Z_1 \frac{Z_{d3} + jZ_1 \tan\theta_{1d}}{Z_1 + jZ_{d3} \tan\theta_{1d}} \quad (5)$$

In (5),  $Z_{d2}$  and  $Z_{d3}$  are given by (6).

$$Z_{d3} = 2Z_2 \frac{Z_{d2} + 2jZ_2 \tan\theta_2}{2Z_2 + jZ_{d2} \tan\theta_2} \quad (6)$$

and,

$$Z_{d2} = -\frac{j(4\pi f_{r,e} C_d Z_2 + \tan\theta_4)}{2\pi f_{r,e} C_d \tan\theta_4} \quad (7)$$

where  $C_d$  denotes the capacitance of IDC. By substituting (4)-(7) in (3) and setting  $Y_{in,e} = 0$ , the even resonance modes ( $f_{r,e}$ ) are found. Based on the derived equation, the proposed resonator is designed to operate in the frequency band of 0.5-2.5 GHz to obtain the capability for measuring BGLs. Table 2 summarizes the dimensions of the proposed resonator. The variations of the first two even modes versus IDC are shown in Figures 4(a) and (b). Figure 4(a) demonstrates that the frequency of the first even mode remains relatively stable with changes in capacitance of IDC. In contrast, Figure 4(b) indicates that selecting a value of  $k$  greater than 0.2 leads to significant variations in the frequency of the second even mode as capacitance of IDC is adjusted. Consequently, the even resonance frequencies of the proposed resonator are dependent on IDC, which typically varies based on the MUT covering the IDC surface. Additionally, the second even mode at 2 GHz exhibits greater sensitivity to changes in IDC compared to the first even mode at 0.8 GHz.

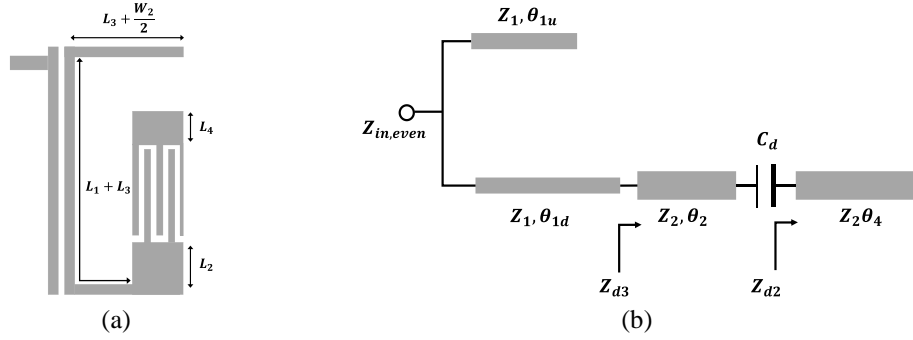


Figure 3. Equivalent circuit model of proposed resonator for even mode: (a) electrical wall and (b) equivalent transmission line model

Table 2. The dimensions of the proposed resonator

Parameter	Size (mm)	Parameter	Size (mm)
$L_0$	2	$W_f$	0.3
$L_1$	20	$W_0$	0.2
$L_2$	5	$W_1$	0.2
$L_3$	10	$W_2$	7.2
$L_4$	2	$g_1$	0.1
$L_f$	5	$g_2$	0.1

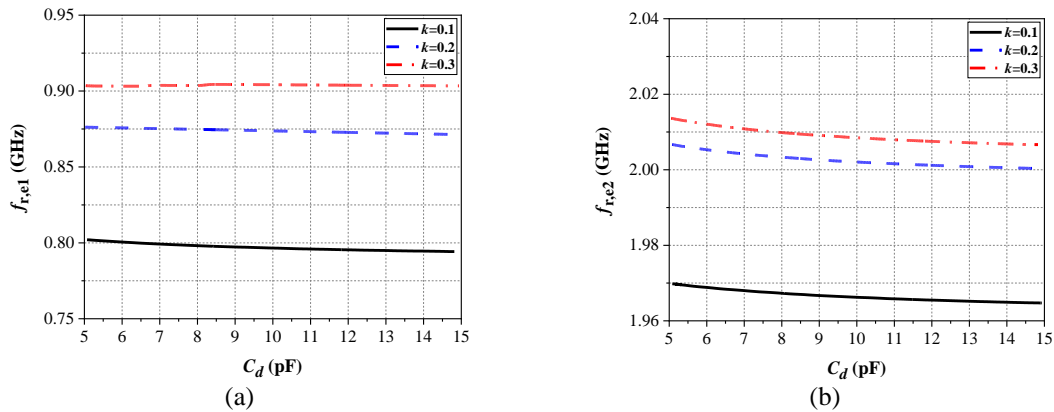


Figure 4. The variation of even resonance frequencies versus IDC at different  $k=Z_2/Z_1$  for (a) the first even mode and (b) the second even mode

### 2.3. Interdigital capacitance characteristics

As shown in Figure 1, the IDC is embedded between the two stubs of the closed-loop square resonator to create a sensitive area for measuring BGLs. Assuming  $L_f \gg W_f$  and  $W_f \gg g_1$ , the total capacitance of IDC is expressed as [29]:

$$C_d = \frac{2\varepsilon_0\varepsilon_{r,eff}L_f(N-1)}{\pi} \ln \left[ \left( 1 + \frac{W_f}{g_1} \right) + \sqrt{\left( 1 + \frac{W_f}{g_1} \right)^2 - 1} \right] \quad (8)$$

where  $N$  and  $\varepsilon_{r,eff}$  represent the number of fingers and effective permittivity of the multilayer microstrip structure, respectively. In the proposed sensor, the fingertip is considered a measurement site. The fingertips can be modeled by a four-layer, as shown in Figure 5 [23]. Table 3 presents the thicknesses and dielectric properties of the four-layer fingertip model.

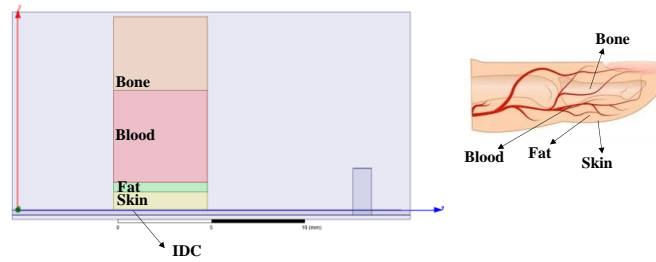


Figure 5. The four-layer model of a fingertip

Table 3. The dielectric properties of the four-layer fingertip model [12], [23]

Layer type	Permittivity	Conductivity (S/m)	Thickness (mm)
Skin	$\epsilon_{r2}=35$	1.562	1
Fat	$\epsilon_{r3}=5.5$	0.103	0.5
Blood	$\epsilon_{r4}=59$	2.503	5
Bone	$\epsilon_{r5}=20$	0.2	4

Consequently, the effective permittivity of the multilayer microstrip IDC is given by [30]:

$$\epsilon_{r,eff} = \epsilon_{r1} + \frac{q_2^2 + q_3^2 + q_4^2 + q_5^2}{\frac{q_2}{\epsilon_{r2}} + \frac{q_3}{\epsilon_{r2}} + \frac{q_4}{\epsilon_{r2}} + \frac{q_5}{\epsilon_{r2}}} \tag{9}$$

where the  $q_i$  are the filling factors, and they depend on the thickness of the layers and finger width.  $\epsilon_{r1}$  is RO6010 substrate permittivity. Dimensions of IDC is determined in such a way that its capacitance in the absence of material samples is equal to  $C_d=10$  pF. According to (9) and (8) and Table 1, it is found that with the increase in BGL, the relative permittivity of human blood decreases, which in turn lowers the capacitance ( $C_d$ ) of the IDC.

### 3. RESULTS AND DISCUSSION

Based on the analytical results, the proposed sensor is designed and simulated using the full-wave electromagnetic (EM) simulator (HFSS). Figure 6(a) shows the sensor simulation setup, while Figure 6(b) depicts the simulated frequency response of the proposed sensor. As seen, the first three resonance frequencies of the proposed sensor occur at 0.73 GHz, 1.24 GHz, and 1.97 GHz, corresponding to the first even mode, first odd mode, and second even mode, respectively.

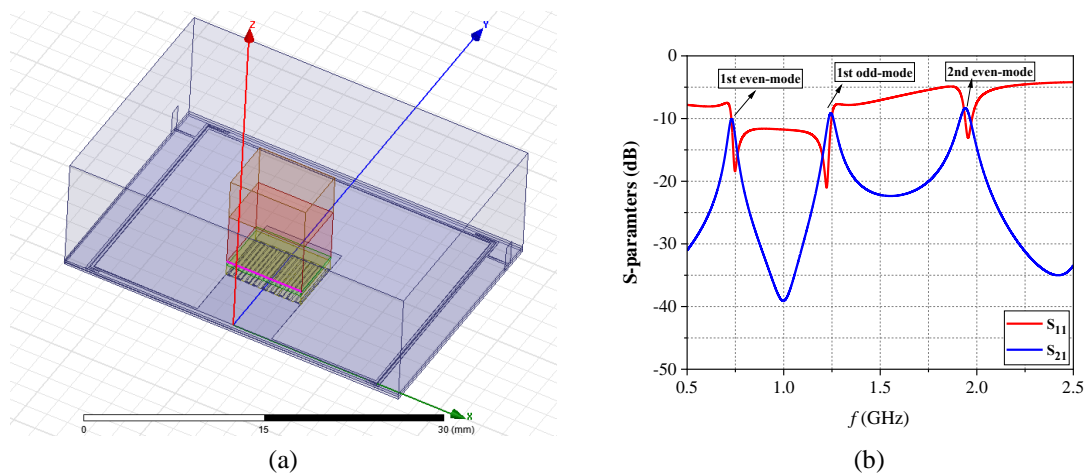


Figure 6. The proposed sensor in the HFSS simulator; (a) the simulation setup and (b) simulated frequency response of the proposed sensor

The measurement of BGLs is based on the resonance frequencies of the proposed sensor. Due to the electromagnetic interaction between the sensor structure and the blood layer with varying permittivity, the change in the S-parameters ( $S_{21}$  or  $S_{11}$ ) can be seen. The simulated  $S_{21}$  of the sensor with five samples of human blood for glucose levels ranging from 0 to 216 mg/dL is shown in Figures 7(a) to (c). As shown in Figure 7(b) and consistent with theoretical analysis, the first odd mode frequency remains unchanged with variations in BGLs. In contrast, Figures 7(a) and (c) demonstrate that the even mode frequency shifts to higher values as BGLs increase. The proposed sensor exhibits a reasonable shift in the even modes, with the  $S_{21}$  peak shifting upward from 1.94 GHz to 1.966 GHz as the BGL increases. As expected, there is no noticeable shift in the first odd mode.

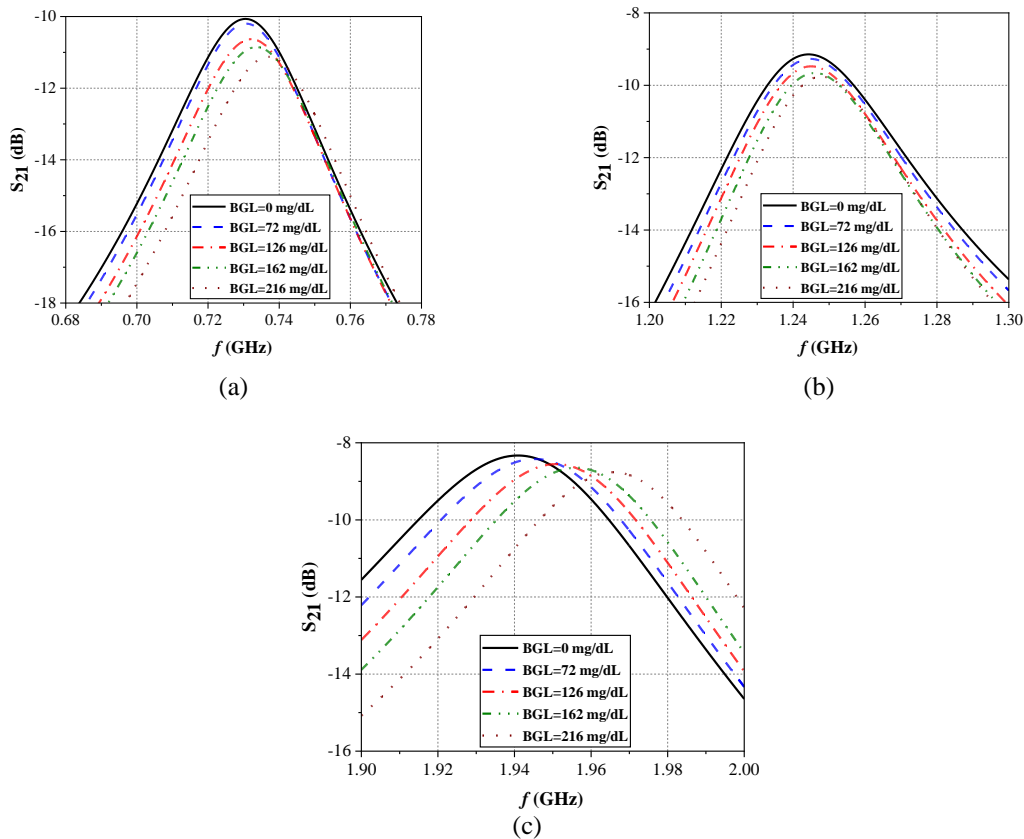


Figure 7. Variation in the resonance frequency with various BGLs at: (a) the first even mode, (b) the first odd mode, and (c) the second even mode

Additionally, the second even mode exhibits greater changes than the first even mode with increasing BGL. The regression analysis between the even resonance frequencies and BGLs is performed as (10) and (11).

$$y_1 = 0.00003x + 0.7294 \quad (10)$$

$$y_2 = 0.00011x + 1.9387 \quad (11)$$

The proposed sensor presents a good linear correlation at the second even mode ( $R^2=0.9485$ ), as shown in Figures 8(a) and (b). Therefore, the sensor reveals a high sensitivity of 110 kHz per mg/dL for the second even mode. The simulated electromagnetic field distribution at the second even resonance frequency of 1.94 GHz is shown in Figures 9(a) and (b). As can be seen, the electromagnetic distribution is higher in skin and fat, while it decreases in the blood region. In addition, at this resonant frequency, the electric field is more concentrated in the sensing region than the magnetic field.

Table 4 provides a comprehensive comparison of the performance characteristics of the proposed sensor against several state-of-the-art sensors, emphasizing key differentiators such as operating frequency, application procedure, and sensitivity.

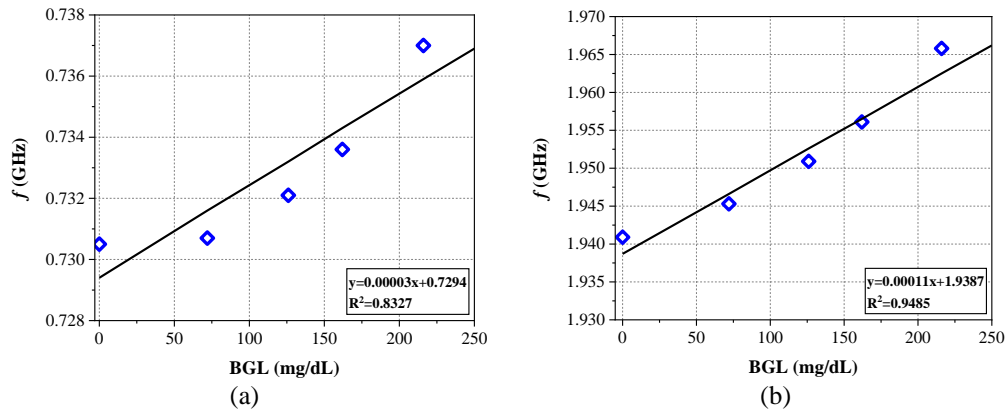


Figure 8. Linear fit of the relationship between even resonance frequencies and BGLs at: (a) the first even mode and (b) the second even mode

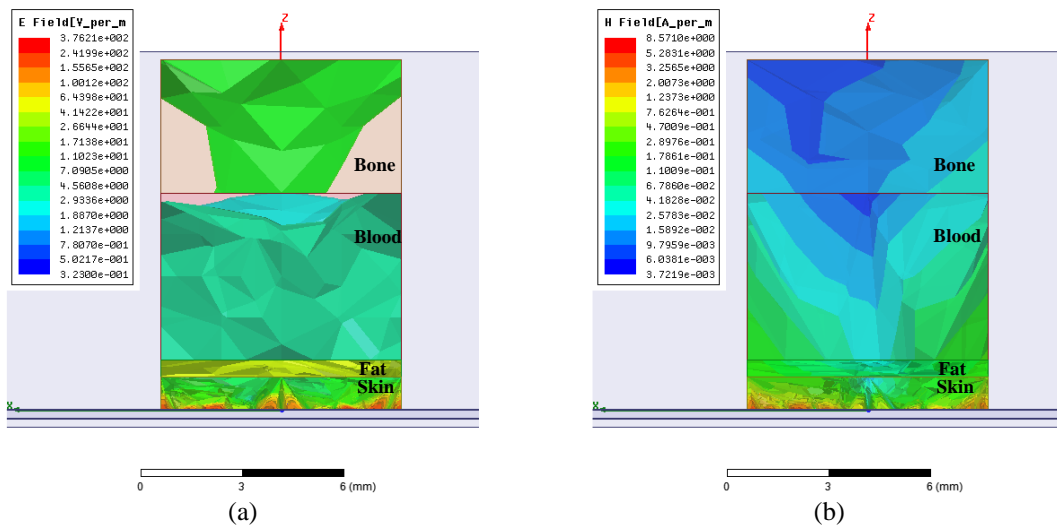


Figure 9. The electromagnetic field distribution over the sensing region at the resonance frequency of 1.94 GHz: (a) electric field distribution and (b) magnetic field distribution

Table 4. The comparison study of the proposed glucose sensor with those previously reported

Ref.	Operating frequency (GHz)	Sensing parameter	Glucose concentration (mg/dL)	Application procedure	Sensitivity (MHz per mg/dL)
[21]	1	$f_r, S_{11}$	148-228	Invasive (serum samples)	1.99
[22]	4.18	$f_r, S_{21}$	0-5000	Invasive (glucose solution)	$2.6 \times 10^{-2}$
[23]	3.4	$f_r, S_{11}$	0-1000	Non-invasive (fingertip)	$1.4 \times 10^{-2}$
[24]	1	$f_r, S_{11}$	30-500	Invasive (glucose solution)	1.17
[25]	4	$f_r, S_{11}$	0-10000	Invasive (glucose solution)	$2.35 \times 10^{-3}$
[31]	4	$f_r, S_{21}$	0-540	Non-invasive (skin tape)	$2.1 \times 10^{-3}$
[32]	2.45	$f_r, S_{11}$	0-400	Invasive (glucose solution)	$2.55 \times 10^{-4}$
[33]	2.45	$f_r, S_{21}$	40-140	Invasive (glucose solution)	$65 \times 10^{-2}$
[34]	9	$f_r, S_{21}$	148-268	Invasive (human serum)	1.08
[35]	2.5	$f_r, S_{11}$	500-8000	Invasive (glucose solution)	$5 \times 10^{-3}$
[36]	0.8, 3.2	$f_r, S_{11}$	25-300	Invasive (glucose solution)	1.38
[26]	5.7	$f_r, S_{11}$	0-900	Non-invasive (glucose solution)	$8.9 \times 10^{-2}$
[37]	2.32	$TZ, S_{21}$	89-456	Non-invasive (fingertip)	$95 \times 10^{-2}$
[27]	2.395	$TZ, S_{21}$	67-400	Non-invasive (fingertip)	$72 \times 10^{-2}$
[38]	2.45	$f_r, S_{11}$	0-500	Non-invasive (fingertip)	$17 \times 10^{-2}$
This work	2	$f_r, S_{21}$	0-216	Non-invasive (fingertip)	$11 \times 10^{-2}$

This comparison not only highlights the technical capabilities of the proposed sensor but also situates it within the broader context of current technologies used for BGL measurement. In terms of operating frequency, the proposed sensor demonstrates a frequency range that is both suitable for effective glucose measurement and conformance to existing technological standards. The choice of an optimal operating frequency is crucial, as it influences the sensor's response time and sensitivity to glucose concentration variations. The findings indicate that the proposed sensor operates efficiently, facilitating rapid measurements without compromising accuracy. The application procedure utilized by the sensor is a critical factor in its assessment. Notably, both the proposed sensor and those referenced in studies [23], [31] employ non-invasive methods for measuring BGLs. This is a significant advantage, as non-invasive techniques minimize patient discomfort and reduce the risk of complications associated with invasive methods, such as infections or scarring. Conversely, other sensors compared in this table rely on aqueous solutions to ascertain glucose levels, categorizing them as invasive procedures. This distinction is vital for users who prioritize comfort and safety in glucose monitoring products. When examining sensitivity, the proposed sensor stands out among its non-invasive counterparts. High sensitivity is essential for accurately detecting minute changes in BGLs, which is particularly crucial for individuals managing diabetes. The data reflect that the proposed sensor exhibits superior sensitivity compared to other resonant-based glucose sensors, making it a promising option for both clinical and personal use. Enhanced sensitivity not only improves the reliability of measurements but also allows for better management of glucose levels, ultimately benefiting the end-user's health and well-being. Furthermore, the overall performance of the proposed sensor reinforces its viability as an innovative alternative in the realm of glucose monitoring. By effectively combining non-invasive measurement techniques with high sensitivity, the proposed sensor addresses two of the most significant drawbacks associated with traditional invasive methods. As a result, it holds the potential to improve patient adherence to monitoring regimens, leading to better health outcomes. In the future, it will be important to explore how this sensor can be integrated with current health monitoring systems, including smartphones, fitness trackers, and electronic health records. This integration has the potential to improve diabetes management by offering real-time access to data and analytical insights.

#### 4. CONCLUSION

This paper presents a resonant-based glucose sensor composed of a closed-loop square resonator integrated with an IDC. The proposed sensor offers a non-invasive method for measuring BGLs by utilizing the dielectric properties of blood at the fingertip. Theoretical analysis and subsequent simulations conducted using ANSYS-HFSS revealed that the second even resonance frequency shifts by approximately 110 kHz for standard BGLs. Additionally, the sensor demonstrates a sensitivity of 110 kHz per mg/dL, surpassing that of existing non-invasive glucose sensors. These findings confirm the sensor's capability for accurately monitoring blood glucose levels. Importantly, the study validates the non-invasive characteristic of the sensor, emphasizing its ability to collect glucose data without the need for blood samples, thereby enhancing patient comfort and compliance. Future research could focus on optimizing the design of the proposed sensor for improved sensitivity. Investigating the effects of temperature and environmental factors on sensor performance will be essential to ensure reliable readings under varying conditions. Furthermore, integrating advanced signal processing techniques may enhance accuracy in real-time glucose monitoring. Exploratory studies could also evaluate the sensor's applicability in continuous glucose monitoring systems, potentially leading to innovations in diabetes management.

#### ACKNOWLEDGMENTS

We would like to express our sincere gratitude to Dr. Akramian for his invaluable assistance and expertise in addressing medical questions related to glucose levels and diabetes management. His guidance has significantly enhanced the quality of our research and provided us with a deeper understanding of the clinical implications of our study.

#### FUNDING INFORMATION

Authors state no funding involved.

#### AUTHOR CONTRIBUTIONS STATEMENT

This journal uses the Contributor Roles Taxonomy (CRediT) to recognize individual author contributions, reduce authorship disputes, and facilitate collaboration.

Name of Author	C	M	So	Va	Fo	I	R	D	O	E	Vi	Su	P	Fu
Abolfazl Bijari	✓	✓		✓	✓	✓	✓		✓	✓		✓		✓
Faezeh Foolad		✓	✓	✓	✓	✓	✓	✓		✓				
Mohammadreza Khorshidi		✓	✓			✓	✓	✓		✓				

C : Conceptualization

M : Methodology

So : Software

Va : Validation

Fo : Formal analysis

I : Investigation

R : Resources

D : Data Curation

O : Writing - Original Draft

E : Writing - Review &amp; Editing

Vi : Visualization

Su : Supervision

P : Project administration

Fu : Funding acquisition

## CONFLICT OF INTEREST STATEMENT

Authors state no conflict of interest.

## INFORMED CONSENT

We have obtained informed consent from all individuals included in this study.

## ETHICAL APPROVAL

This study did not involve any human participants or animals. Therefore, ethical approval was not required.

## DATA AVAILABILITY

Data availability is not applicable to this paper as no new data were created or analyzed in this study.

## REFERENCES

- [1] W. Gao *et al.*, "Fully integrated wearable sensor arrays for multiplexed in situ perspiration analysis," *Nature*, vol. 529, no. 7587, pp. 509–514, Jan. 2016, doi: 10.1038/nature16521.
- [2] D. R. Whiting, L. Guariguata, C. Weil, and J. Shaw, "IDF diabetes atlas: Global estimates of the prevalence of diabetes for 2011 and 2030," *Diabetes Research and Clinical Practice*, vol. 94, no. 3, pp. 311–321, Dec. 2011, doi: 10.1016/j.diabres.2011.10.029.
- [3] T. Chretiennot, D. Dubuc, and K. Grenier, "Microwave-based microfluidic sensor for non-destructive and quantitative glucose monitoring in aqueous solution," *Sensors*, vol. 16, no. 10, Oct. 2016, doi: 10.3390/s16101733.
- [4] J. Hönes, P. Müller, and N. Surrage, "The technology behind glucose meters: Test strips," *Diabetes Technology & Therapeutics*, vol. 10, no. s1, p. S-10-S-26, Jun. 2008, doi: 10.1089/dia.2008.0005.
- [5] T. Lin, "Non-invasive glucose monitoring: A review of challenges and recent advances," *Current Trends in Biomedical Engineering & Biosciences*, vol. 6, no. 5, Jul. 2017, doi: 10.19080/CTBEB.2017.06.555696.
- [6] S. Laha, A. Rajput, S. S. Laha, and R. Jadhav, "A concise and systematic review on non-invasive glucose monitoring for potential diabetes management," *Biosensors*, vol. 12, no. 11, pp. 965–985, Nov. 2022, doi: 10.3390/bios12110965.
- [7] H. Choi *et al.*, "Design and in vitro interference test of microwave noninvasive blood glucose monitoring sensor," *IEEE Transactions on Microwave Theory and Techniques*, vol. 63, no. 10, pp. 3016–3025, Oct. 2015, doi: 10.1109/TMTT.2015.2472019.
- [8] C. G. Juan, E. Bronchalo, B. Potelon, C. Quendo, and J. M. Sabater-Navarro, "Glucose concentration measurement in human blood plasma solutions with microwave sensors," *Sensors*, vol. 19, no. 17, Aug. 2019, doi: 10.3390/s19173779.
- [9] R. Liu and T. Cui, "Simulation on biomarker sensor miniaturization based on metamaterial," *Modern Physics Letters B*, vol. 33, no. 11, Apr. 2019, doi: 10.1142/S0217984919501355.
- [10] J. Vrba, J. Karch, and D. Vrba, "Phantoms for development of microwave sensors for noninvasive blood glucose monitoring," *International Journal of Antennas and Propagation*, vol. 2015, pp. 1–5, 2015, doi: 10.1155/2015/570870.
- [11] Y. Hayashi, L. Livshits, A. Caduff, and Y. Feldman, "Dielectric spectroscopy study of specific glucose influence on human erythrocyte membranes," *Journal of Physics D: Applied Physics*, vol. 36, no. 4, pp. 369–374, Feb. 2003, doi: 10.1088/0022-3727/36/4/307.
- [12] T. Yilmaz, R. Foster, and Y. Hao, "Broadband tissue mimicking phantoms and a patch resonator for evaluating noninvasive monitoring of blood glucose levels," *IEEE Transactions on Antennas and Propagation*, vol. 62, no. 6, pp. 3064–3075, Jun. 2014, doi: 10.1109/TAP.2014.2313139.
- [13] M. A. H. Ansari, A. K. Jha, and M. J. Akhtar, "Design and application of the CSRR-based planar sensor for noninvasive measurement of complex permittivity," *IEEE Sensors Journal*, vol. 15, no. 12, pp. 7181–7189, Dec. 2015, doi: 10.1109/JSEN.2015.2469683.
- [14] A. E. Omer *et al.*, "Non-invasive real-time monitoring of glucose level using novel microwave biosensor based on triple-pole CSRR," *IEEE Transactions on Biomedical Circuits and Systems*, vol. 14, no. 6, pp. 1407–1420, Dec. 2020, doi: 10.1109/TBCAS.2020.3038589.
- [15] S. Y. Huang *et al.*, "Microstrip line-based glucose sensor for noninvasive continuous monitoring using the main field for sensing and multivariable crosschecking," *IEEE Sensors Journal*, vol. 19, no. 2, pp. 535–547, Jan. 2019, doi: 10.1109/JSEN.2018.2877691.
- [16] X. Li and C. Li, "Research on non-invasive glucose concentration measurement by NIR transmission," in *2015 IEEE International Conference on Computer and Communications (ICCC)*, Oct. 2015, pp. 223–228, doi: 10.1109/CompComm.2015.7387571.
- [17] M. P. Parkhomenko *et al.*, "Analysis of dielectric properties of blood and development of a resonator method for noninvasive measuring of glucose content in blood," *Journal of Communications Technology and Electronics*, vol. 62, no. 3, pp. 267–281, 2017, doi: 10.1134/S1064226917030159.
- [18] H. Cano-Garcia *et al.*, "Reflection and transmission measurements using 60 GHz patch antennas in the presence of animal tissue for

*A new resonant-based sensor for non-invasive measurement of blood glucose levels (Abolfazl Bijari)*

- non-invasive glucose sensing,” in *2016 10th European Conference on Antennas and Propagation (EuCAP)*, Apr. 2016, pp. 1–3. doi: 10.1109/EuCAP.2016.7481178.
- [19] M. Hofmann, M. Bloss, R. Weigel, G. Fischer, and D. Kissinger, “Non-invasive glucose monitoring using open electromagnetic waveguides,” in *2012 42nd European Microwave Conference*, Oct. 2012, pp. 546–549. doi: 10.23919/EuMC.2012.6459152.
- [20] N. Sharafadinzadeh, M. Abdolrazzagh, and M. Daneshmand, “Highly sensitive microwave split ring resonator sensor using gap extension for glucose sensing,” in *2017 IEEE MTT-S International Microwave Workshop Series on Advanced Materials and Processes for RF and THz Applications (IMWS-AMP)*, Sep. 2017, pp. 1–3. doi: 10.1109/IMWS-AMP.2017.8247400.
- [21] N.-Y. Kim, K. K. Adhikari, R. Dhakal, Z. Chuluunbaatar, C. Wang, and E.-S. Kim, “Rapid, sensitive and reusable detection of glucose by a robust radiofrequency integrated passive device biosensor chip,” *Scientific Reports*, vol. 5, no. 1, Jan. 2015, doi: 10.1038/srep07807.
- [22] G. Govind and M. J. Akhtar, “Metamaterial-inspired microwave microfluidic sensor for glucose monitoring in aqueous solutions,” *IEEE Sensors Journal*, vol. 19, no. 24, pp. 11900–11907, Dec. 2019, doi: 10.1109/JSEN.2019.2938853.
- [23] V. Turgul and I. Kale, “Simulating the effects of skin thickness and fingerprints to highlight problems with non-invasive RF blood glucose sensing from fingertips,” *IEEE Sensors Journal*, vol. 17, no. 22, pp. 7553–7560, Nov. 2017, doi: 10.1109/JSEN.2017.2757083.
- [24] A. Kumar *et al.*, “High-sensitivity, quantified, linear and mediator-free resonator-based microwave biosensor for glucose detection,” *Sensors*, vol. 20, no. 14, Jul. 2020, doi: 10.3390/s20144024.
- [25] Z. Abedeen and P. Agarwal, “Microwave sensing technique based label-free and real-time planar glucose analyzer fabricated on FR4,” *Sensors and Actuators A: Physical*, vol. 279, pp. 132–139, Aug. 2018, doi: 10.1016/j.sna.2018.06.011.
- [26] T. Singh, P. K. Mishra, A. Pal, and V. S. Tripathi, “A planar microwave sensor for noninvasive detection of glucose concentration using regression analysis,” *International Journal of Microwave and Wireless Technologies*, vol. 15, no. 8, pp. 1343–1353, Oct. 2023, doi: 10.1017/S1759078723000545.
- [27] P. Mohammadi, A. Mohammadi, S. Demir, and A. Kara, “Compact size, and highly sensitive, microwave sensor for non-invasive measurement of blood glucose level,” *IEEE Sensors Journal*, vol. 21, no. 14, pp. 16033–16042, Jul. 2021, doi: 10.1109/JSEN.2021.3075576.
- [28] J. Venkataraman and B. Freer, “Feasibility of non-invasive blood glucose monitoring: In-vitro measurements and phantom models,” in *2011 IEEE International Symposium on Antennas and Propagation (APSURSI)*, Jul. 2011, pp. 603–606. doi: 10.1109/APS.2011.5996782.
- [29] S. C. Mukhopadhyay, B. George, J. K. Roy, and T. Islam, Eds., *Interdigital sensors: Progress over the last two decades*, vol. 36. Cham: Springer International Publishing, 2021. doi: 10.1007/978-3-030-62684-6.
- [30] J. Svacina, “A simple quasi-static determination of basic parameters of multilayer microstrip and coplanar waveguide,” *IEEE Microwave and Guided Wave Letters*, vol. 2, no. 10, pp. 385–387, Oct. 1992, doi: 10.1109/75.160115.
- [31] M. Baghelani, Z. Abbasi, M. Daneshmand, and P. E. Light, “Non-invasive continuous-time glucose monitoring system using a chipless printable sensor based on split ring microwave resonators,” *Scientific Reports*, vol. 10, no. 1, Jul. 2020, doi: 10.1038/s41598-020-69547-1.
- [32] Satish, K. Sen, and S. Anand, “Demonstration of microstrip sensor for the feasibility study of non-invasive blood-glucose sensing,” *MAPAN*, vol. 36, no. 1, pp. 193–199, Mar. 2021, doi: 10.1007/s12647-020-00396-z.
- [33] A. E. Omer *et al.*, “Low-cost portable microwave sensor for non-invasive monitoring of blood glucose level: novel design utilizing a four-cell CSRR hexagonal configuration,” *Scientific Reports*, vol. 10, no. 1, Sep. 2020, doi: 10.1038/s41598-020-72114-3.
- [34] N. Y. Kim, R. Dhakal, K. K. Adhikari, E. S. Kim, and C. Wang, “A reusable robust radio frequency biosensor using microwave resonator by integrated passive device technology for quantitative detection of glucose level,” *Biosensors and Bioelectronics*, vol. 67, pp. 687–693, May 2015, doi: 10.1016/j.bios.2014.10.021.
- [35] A. Ebrahimi, J. Scott, and K. Ghorbani, “Microwave reflective biosensor for glucose level detection in aqueous solutions,” *Sensors and Actuators A: Physical*, vol. 301, Jan. 2020, doi: 10.1016/j.sna.2019.111662.
- [36] W. Yue, E.-S. Kim, B.-H. Zhu, J. Chen, J.-G. Liang, and N.-Y. Kim, “Permittivity-inspired microwave resonator-based biosensor based on integrated passive device technology for glucose identification,” *Biosensors*, vol. 11, no. 12, Dec. 2021, doi: 10.3390/bios11120508.
- [37] P. Mohammadi, A. Mohammadi, and A. Kara, “Dual-frequency microwave resonator for noninvasive detection of aqueous glucose,” *IEEE Sensors Journal*, vol. 23, no. 18, pp. 21246–21253, Sep. 2023, doi: 10.1109/JSEN.2023.3303170.
- [38] R. W. Aldhaheri, J. B. Kamili, A. Nella, and N. M. Sobahi, “A novel compact highly sensitive non-invasive microwave antenna sensor for blood glucose monitoring,” *Open Physics*, vol. 21, no. 1, Sep. 2023, doi: 10.1515/phys-2023-0107.

## BIOGRAPHIES OF AUTHORS



**Abolfazl Bijari**    He was born in Birjand, Iran, in 1982. He earned his B.S. in Telecommunication Engineering in 2005, followed by an M.S. in Electronics Engineering in 2007, and a Ph.D. in Electronics Engineering in 2013, all from Ferdowsi University of Mashhad (FUM), Iran. Currently, he is an Associate Professor in the Department of Electronics Engineering at the University of Birjand, Iran. His research interests include RFIC design, microwave filters, and MEMS-based devices. He can be contacted at email: a.bijari@birjand.ac.ir.



**Faeze Foolad**    was born in Mashhad, Iran in 1998. She received B.S. and M.S. degree in Electronics Engineering from Khayyam University and University of Birjand, Iran in 2019, 2022, respectively. Currently, she is a lecturer in Department of Electronics Engineering, Khayyam University, Mashhad, Iran. His current research interests include Microwave-based sensor and RF circuit design. She can be contacted at email: Faezeh.foolad@birjand.ac.ir.



**Mohammadreza Khorshidi**    was born in Iran. He received the Master of Science (M.Sc.) degree in 2009 from K.N. Toosi University of Technology and Ph.D. degree in Communication Engineering in Shahed University, Iran. He is currently an Assistant Professor with the Department of Electrical Engineering, University of Birjand, Iran. His main research interest is terahertz technology with focus on photoconductive antennas and plasmonic structures. He can be contacted at email: mkhorshidi@birjand.ac.ir.